Variation of TNF modulates cellular immunity of gregarious and solitary locusts against fungal pathogen *Metarhizium anisopliae*

Yundan Wang[a], Xiwen Tong[a], Shenglei Yuan[a], Pengcheng Yang[b], Ling Li[c], Yong Zhao[c], and Le Kang[a,b,1]

[a]State Key Laboratory of Integrated Management of Pest Insects and Rodents, Institute of Zoology, Chinese Academy of Sciences, Beijing 100101, China; [b]Beijing Institutes of Life Science, Chinese Academy of Sciences, Beijing 100101, China; and [c]State Key Laboratory of Biomembrane and Membrane Biotechnology, Institute of Zoology, Chinese Academy of Sciences, Beijing 100101, China

Contributed by Le Kang; received November 16, 2021; accepted December 28, 2021; reviewed by Jens Rolff and Sibao Wang

Changes in population density lead to phenotypic differentiation of solitary and gregarious locusts, which display different resistance to fungal pathogens; however, how to regulate their cellular immune strategies remains unknown. Here, our stochastic simulation of pathogen proliferation suggested that humoral defense always enhanced resistance to fungal pathogens, while phagocytosis sometimes reduced defense against pathogens. Further experimental data proved that gregarious locusts had significantly decreased phagocytosis of hemocytes compared to solitary locusts. Additionally, transcriptional analysis showed that gregarious locusts promoted immune effector expression (*gnbp1* and *dfp*) and reduced phagocytic gene expression (*eater*) and the cytokine tumor necrosis factor (TNF). Interestingly, higher expression of the cytokine TNF in solitary locusts simultaneously promoted *eater* expression and inhibited *gnbp1* and *dfp* expression. Moreover, inhibition of TNF increased the survival of solitary locusts, and injection of TNF decreased the survival of gregarious locusts after fungal infection. Therefore, our results indicate that the alerted expression of TNF regulated the immune strategy of locusts to adapt to environmental changes.

ecological immunology | tumor necrosis factor | cellular defenses | density-dependent prophylaxis

From biblical times to 2020, the locust is the most destructive migratory pest on crops, pasture, and fodder because it is highly mobile and can form swarms containing millions of locusts in various parts of Africa, Asia, and the Middle East. Population density is an important ecological factor that affects physiological processes in animal species. High population density is an important factor that facilitates collective survival in animal groups (1, 2). Locusts (*Locusta migratoria*) exhibit a remarkable density-dependent polyphenism, for which changes in population density are the key factors driving the transition between solitary and gregarious phases accompanied by considerable phenotypic, physiological, and gene expression variations (3, 4). Recent studies have recognized that immunity is dynamic and adapts to environmental variations and opportunities (5–7). A previous study showed that crowded conditions stimulate the migratory locusts to divert their molecular immune strategies against pathogens and cause density-dependent prophylactic immunity for population survival (3). Expression profiles in the fat bodies of locusts reveal that gregarious locusts enhance pattern recognition proteins to sequester pathogens and increase the Euclidean distance between infectious and healthy individuals (3). Interestingly, the cellular defenses of invertebrate animals often use phagocytosis, encapsulation, and nodulation to sequester and eliminate pathogens.

Our previous studies have demonstrated that the migratory locusts can respond to changes in population density in the global profiles of coding genes, microRNA transcription, and metabolomes, so that manipulating them can lead to significant changes in locust phenotypes (8–11). Gregarious locusts display significantly stronger resistance to fungal pathogens than solitary locusts do at the molecular immune level (2, 3). Although the encapsulation and total hemocyte counts did not show a significant difference between solitary and gregarious desert locusts, differential cellular defenses have been investigated by enumerating hemocytes in other insect species (12). However, recent studies have revealed an inconsistent release of sessile hemocytes into hemocoel circulation in mosquitoes during infections (13, 14). Despite the number of hemocytes, cellular defenses can modulate the systematic responses of hosts by secreting cytokines (15, 16). Importantly, altered immunity in invertebrates is modulated by various cytokines, including growth-blocking peptides (GBPs), unpaired proteins (Upds), PDGF/VEGF-receptor related protein (Pvr), and eiger/tumor necrosis factor (TNF) (17–20). In particular, TNF can regulate comprehensive changes in physiology, including energy consumption (21), phagocytosis, and immune effector production (22–24). However, the role of cellular defenses in density-dependent prophylactic immunity remains largely unknown.

To understand the interactions between hemocytes and microbes, stochastic simulations were applied to investigate the kinetic proliferation of microbes under various conditions. The

Significance

Ecological immunology addresses the interactions between host immunity and the environment. Locusts display density-dependent phase transitions between solitary and gregarious locusts. In control practices and laboratory bioassays, gregarious locusts always exhibit stronger resistance to fungal pathogens than solitary locusts. However, few studies have investigated the mechanism of altered immune switch in locusts. Here, we combined mathematical simulation and experimental studies to show that gregarious locusts inhibit tumor necrosis factor (TNF) to alter immune defense by enhancing humoral defense and reducing cellular defense, and high levels of TNF reduce the survival of solitary locusts. Our study provides an important cue for understanding cellular immunity variations in response to different population densities and for improving the control efficacy of locust plagues.

Author contributions: Y.W. and L.K. designed research; Y.W., X.T., and S.Y. performed research; X.T., S.Y., and L.K. contributed new reagents/analytic tools; Y.W., X.T., P.Y., L.L., and L.K. analyzed data; and Y.W., Y.Z., and L.K. wrote the paper.

Reviewers: J.R., Freie Universität Berlin; and S.W., Chinese Academy of Sciences.

The authors declare no competing interest.

[1]To whom correspondence may be addressed. Email: lkang@ioz.ac.cn.

This article contains supporting information online at http://www.pnas.org/lookup/suppl/doi:10.1073/pnas.2120835119/-/DCSupplemental.

Published February 2, 2022.

prescription of these mathematical models is an enumeration of the possible events and how their rates depend on parameters and the current state of the system (25). Given the parameters and their values, numerical solutions were generated using the Gillespie algorithm (26, 27). Simple stochastic models of kinetic variations between cell and pathogen populations are the birth–death process. The death rates of pathogens are dependent on immune cell phagocytosis, humoral attack, and natural death. The death of immune cells depends on the rates of phagocytosis, recovery, destruction, and natural death. By describing the variable immune defenses computationally, we can gain a deep insight into processes that are not accessible through experimental means.

In this study, we combined the mathematical model with experiments to compare the differential phagocytic abilities of gregarious and solitary locust hemocytes. We used transcriptome analysis to investigate the critical cytokines involved in regulating the altered immunity of locusts. Finally, we observed that cytokines regulate the survival of locusts after infection with the fungal pathogen, *Metarhizium anisopliae*. Our study found that TNF functions as a switch to alert the cellular immune strategy of solitary and gregarious locusts against infection by a fungal pathogen, providing cytological evidence for ecological immunity of density-dependent and important cues for improving the efficiency of biological control of locusts.

Results

Differential Effects of Humoral and Cellular Defenses against Pathogen Growth. To understand the kinetics of the immune response during infection, we used the stochastic model (26, 27), which enumerates the possible events, to simulate the kinetics of microbial growth and hemocyte survival (Fig. 1*A*).

At an infinitely small interval of Δt time, the total functional hemocytes are the sum of self-renewal, survival of hemocytes, and minus of phagocytes (assumed as one hemocyte eats one microbe), and the total of free microbes is the sum of self-renewal, survival of microbes, and minus of phagocytes. The kinetics of hemocyte and microbe proliferation are described by ordinary differential Eqs. **1** and **2**:

$$\mathrm{d(hemocytes)/dt} = \alpha * \mathrm{N} + (\mathrm{K2} - 1)\mathrm{K1} * \mathrm{M} * \mathrm{N} \qquad [1]$$

$$\mathrm{d(microbes)/dt} = \beta * \mathrm{M} + (\mathrm{K3} - 1) * \mathrm{K1} * \mathrm{M} * \mathrm{N} \qquad [2]$$

Here, α indicates the increased rate of hemocytes for the total events of proliferation, migration, and death, and β indicates the increased rate of microbes, including the total events of proliferation and death by humoral attack. K1, K2, and K3 indicate the rate of phagocytosis efficiency, phagocyte recovery, and phagocyte death (microbe escape), respectively (Fig. 1*A*). In addition, N and M indicate the initial number of hemocytes and microbes in the system, respectively. Herein, we assume that one hemocyte engulfed microbes with high efficiency from 20 to 100%, representing regular and enhanced cellular defense. By observing humoral defense, we used the low growth rate of microbes to present enhanced humoral defense. According to a previous study on humoral defense in gregarious locusts, we assumed a 1.5-fold in the growth rate of microbes to present regular humoral defense of hosts compared to enhanced humoral defenses. Moreover, here, we assumed a phagocyte recovery rate K2 = 0.2 as high virulent pathogens, and K2 = 0.8 as low virulent pathogens. At a given time point, the sum of the K2 and K3 rates is 1.0. To investigate the different status of virulence of pathogens, enhanced humoral and cellular defenses, we conducted total 8 statuses for comparing the hemocytes survival time and microbe elimination time (Fig. 1*B* and Table 1).

Although both enhanced humoral and cellular defenses can eliminate low virulence microbes within the shortest time (status 2), the host showed a shorter survival time with high virulence microbial infection (status = 3, t = 5.947, $n = 0$) (Fig. 1*C*, *Left*) than the host with low cellular defense and enhanced humoral defense (status 6, t = 6.752, $n = 0$) (Fig. 1*D*, *Left*). These results suggested that enhanced cellular and humoral defenses did not always benefit the hosts.

Interestingly, enhanced humoral defense with low cellular defense costs more time to eliminate low-virulence microbes (status = 8, t = 6.01, M = 0) (Fig. 1*D*, *Right*) compared to enhanced cellular defense with low humoral defense (status = 4, t = 2.788, M = 0) (Fig. 1*C*, *Right*). The stochastic simulation indicated that enhanced humoral with low cellular defenses provides the optimal strategy for host survival during high-virulence pathogen infection despite an extended interaction between the host and low-virulence microbes.

Gregarious Locusts Reduced Phagocytosis. To verify the strategy of optimal immunity in gregarious and solitary locusts, we compared the differences in cellular defenses between them (Fig. 2*A*). Flow cytometry was used to examine the proportion and capacity of phagocytes after injection with fluorescein isothiocyanate (FITC)-labeled conidia of *M. anisopliae* (Fig. 2*B*). Gregarious locusts showed a lower phagocytic ability than solitary locusts after counting the same hemocytes at different concentrations of fungal conidia (Fig. 2*C* and *SI Appendix*, Fig. S1*A*). Moreover, the differential phagocytic ability was evaluated by comparing FITC intensity. Gregarious locusts showed a significantly lower proportion of hemocytes (4.68 ± 1.48%) than solitary locusts (10.35 ± 1.94%, $n = 12$, $P < 0.001$) (Fig. 2*D*), and gregarious locusts also showed a lower FITC mean value (342 ± 58.68) than solitary locusts (544.12 ± 52.56, $n = 12$, $P < 0.001$) (Fig. 2*D*). Furthermore, an in vitro phagocytosis assay was used to observe the phagocytic ability of adherent hemocytes, which are mostly plasmatocytes, showing that gregarious locusts reduced phagocytosis ($n = 44$, $P = 0.026$) (*SI Appendix*, Fig. S1 *B–D*). Thus, the hemocytes of gregarious locusts exhibited significantly lower phagocytic ability than those of solitary locusts. Combined with model simulation, gregarious locusts employed a defense strategy of low cellular defenses, whereas solitary locusts preferred enhanced cellular defenses.

Gregarious Locusts Enhanced the Expression of Effectors. To understand the mechanism of distinct cellular defenses in locusts, we conducted transcriptome analysis to investigate the gene expression profiles in solitary and gregarious locusts. Transcriptome sequencing of pre- and postinfected locusts by the pathogenic fungus *M. anisopliae* generated >140 million paired-end reads. Differentially expressed genes (DEGs) were analyzed using the DEGseq software after alignment of reads to the locust reference genome (28). Among these genes, 552 and 326 were uniquely regulated in infected solitary and gregarious locusts, respectively (Fig. 3*A*).

Hierarchical clustering analysis of the total DEGs (1,990 genes, q-value < 0.05, $P < 0.001$) showed that hemocytes of solitary and gregarious locusts exhibited significantly different patterns of gene expression, implying different defense strategies (Fig. 3*B*). In the upper cluster, gregarious hemocytes prophylactically employed immune genes, including *defense proteins*, *serine proteases*, *lysozyme*, and *gram-negative binding protein1* (*gnbp1*), to fight against fungal infection; in the lower cluster, the hemocytes of solitary locusts prophylactically employed genes, including *eater*, *tumor necrosis factor* (*tnf*), and *pirk*, to resist infection (Fig. 3*B* and *SI Appendix*, Tables S1 and S2). Importantly, hemocytes of solitary locusts highly expressed the lipopolysaccharide (LPS)-induced tumor necrosis factor alpha factor (LITA) gene (*SI Appendix*, Table S1), which can induce

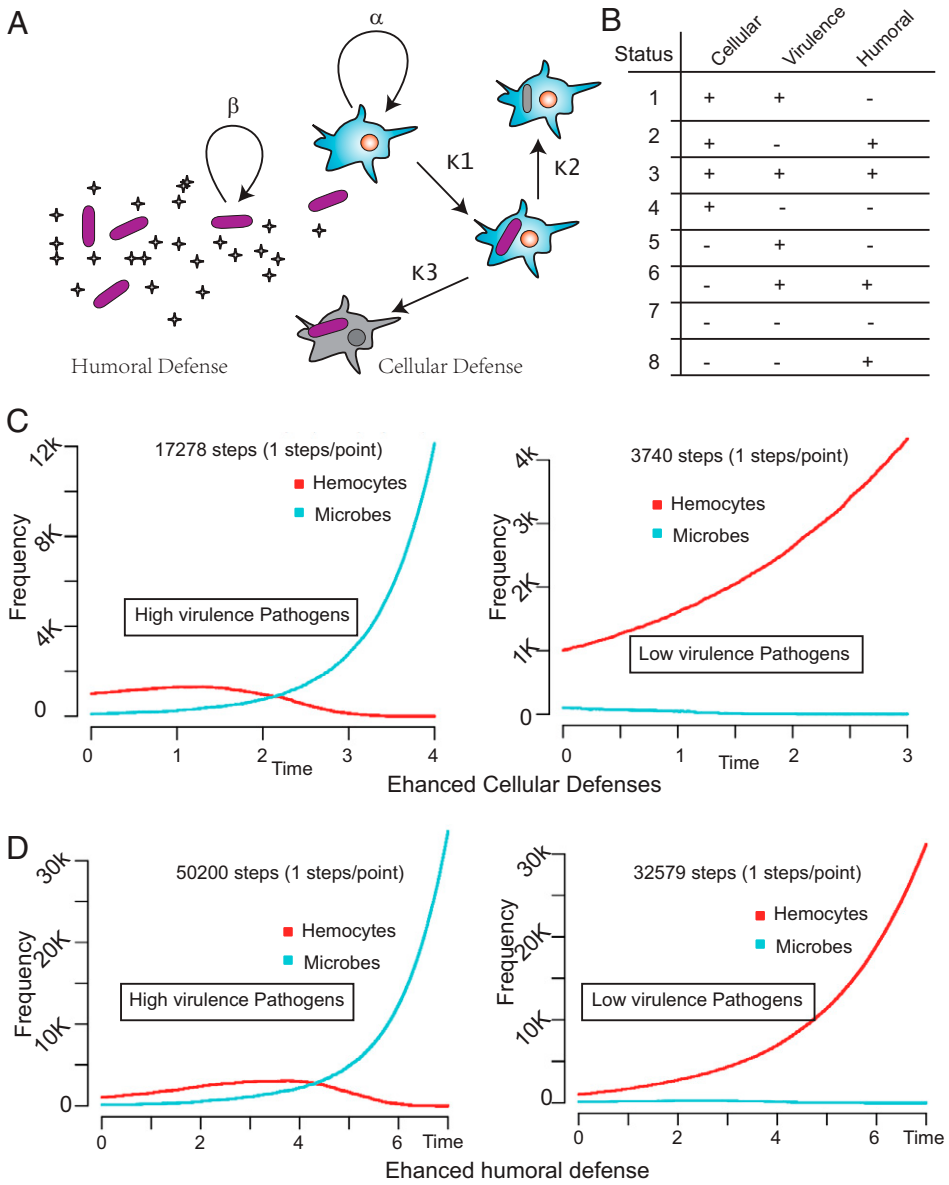

Fig. 1. Stochastic simulation of hemocytes and pathogen growth in altered immune defenses. (*A*) The schematic of humoral and cellular defense in host resist pathogen infection. α indicates the increase rate of hemocytes for the total events of the proliferation, migration, and death, and β indicates the increase rate of microbes including the total events of the proliferation and death by humoral attack. K1, K2, and K3 indicates the rate of phagocytosis efficient, phagocytes recovery, and phagocytes death (microbe escape) respectively. (*B*) To observe the competence of hemocytes and microbe growth, various status of cellular defense, microbe virulence and humoral defenses were examined in simulation. All status (8 combinations) of cellular defense, humoral defense, and microbe virulence (high or low) were observed in the simulation. (*C*) Kinetic curves of hemocytes and microbes by immune defense of high humoral and high cellular defenses. *Left* indicates status 3 and *Right* indicates status 4. (*D*) Kinetic curves of hemocytes and microbes by immune defense of high humoral and low cellular defenses. *Left* indicates status 6 and *Right* indicates status 8.

TNF expression. *Pirk* encodes gene of negative regulator of IMD pathway in respond to gram-negative bacteria, and LITAF was induced by LPS from gram-negative bacteria. These results implied that solitary locusts may have large amounts of gram-negative bacteria.

Analysis of the differentially expressed genes of hemocytes in solitary and gregarious locusts in response to fungal infection and gene ontology (GO) enrichment showed that hemocytes of gregarious locusts preferred hydrolysis activity, while hemocytes of solitary locusts used biological processes, including cell communication, signal transduction, and single organism signaling (*SI Appendix*, Table S3). At the basal differentially expressed genes between hemocytes of solitary and gregarious locusts, gene ontology enrichment showed that hemocytes of gregarious locusts applied catalytic activity, including peptidoglycan and glycosaminoglycan, while hemocytes of solitary locusts preferred transport activity (*SI Appendix*, Table S2).

qPCR of selected differentially expressed genes confirmed the results of transcriptome analysis ($r^2 = 0.93$) (*SI Appendix*, Table S3). Furthermore, gregarious locusts prophylactically expressed the immune effector *gnbp1* ($n = 12$, $P = 0.0102$) and *defense protein* (*dfp*) ($n = 12$, $P < 0.001$) in hemocytes in response to fungal infection (Fig. 3*C*). In addition, there was no significant difference in the expression of antimicrobial peptides (AMPs) ($n = 12$, $P = 0.435$) between solitary and gregarious locusts (Fig. 3*C*). Among various receptors for phagocytosis including PGRP-LE, draper and nimrod, receptor *eater* expression of solitary locusts showed higher level compared to

Table 1. Parameters for stochastic simulation of hemocytes and microbe growth

Status	1	2	3	4	5	6	7	8
K1	0.001	0.001	0.001	0.001	0.0002	0.0002	0.0002	0.0002
K2	0.2	0.8	0.2	0.8	0.2	0.2	0.8	0.8
K3	0.8	0.2	0.8	0.2	0.8	0.8	0.2	0.2
α	0.5	0.5	0.5	0.5	0.5	0.5	0.5	0.5
β	1.5	1	1	1.5	1.5	1	1.5	1
N	1,000	1,000	1,000	1,000	1,000	1,000	1,000	1,000
M	100	100	100	100	100	100	100	100
Enhance cellular	Yes	Yes	Yes	Yes	No	No	No	No
Pathogen virulence	Yes	No	Yes	No	Yes	Yes	No	No
Enhance humoral	No	Yes	Yes	No	No	Yes	No	Yes
N (0, t)	3.616	n/a	5.947	n/a	4.381	6.752	n/a	n/a
M (0, t)	n/a	1.784	n/a	2.788	n/a	n/a	6.507	6.01

We assumed that initial number of hemocytes was 1,000 and the initial number of microbes was 100. N (0, t) means that the hemocytes number is zero at time of t, indicating the failure of immune defense of hosts; M (0, t) means that the microbes number is zero at time of t, indicating the elimination of microbes; n/a means that data is not available in simulation procedures because hemocytes or microbes are eliminated by their competence.

gregarious locusts ($n = 12$, $P = 0.0002$) (Fig. 3*D*). Because the hemocytes of solitary locusts express the TNF inducer LITAF at a highly basal level, TNF plays a vital role in regulating the optimal defense of locusts in response to density changes. Furthermore, we observed that solitary locusts increased the cytokine *tnf* for the phosphorylation of c-Jun N-terminal kinase (JNK) (Fig. 3*E*). These results suggest that TNF modulates the receptor and effectors to regulate cellular defenses of locusts.

Cytokine TNF Simultaneously Enhanced Phagocytosis and Reduced the Effector Expression of Hemocytes. Based on phylogenetic analysis, locust TNF was clustered into a clade of *eigers* of *Drosophila*. Furthermore, we successfully knocked down *tnf* and *eater* expression in the hemocytes (Fig. 4*A*). Knockdown of *tnf* significantly decreased *eater* expression ($n_S = 12$, $P_S = 0.0002$) and increased *gnbp1* expression ($n_S = 12$, $P_S = 0.003$) in the hemocytes of solitary locusts (Fig. 4*B*). Knockdown of *tnf* decreased the proportion of phagocytic cells in solitary locusts ($n_S = 12$, $P_S = 0.017$, but did not affect their phagocytic capacity (Fig. 4*C*). Knockdown of *eater* significantly decreased the proportion of phagocytes ($n_S = 12$, $P_S = 0.0315$) but did not affect the capacity of phagocytes (Fig. 4*D*). Improvement in TNF levels by injection of purified recombinant TNF protein into gregarious locusts significantly reduced *gnbp1* production ($n_G = 12$, $P_G < 0.001$) and promoted *eater* expression ($n_G = 12$, $P_G = 0.0022$) (Fig. 4*E*). Moreover, recombinant TNF increased the

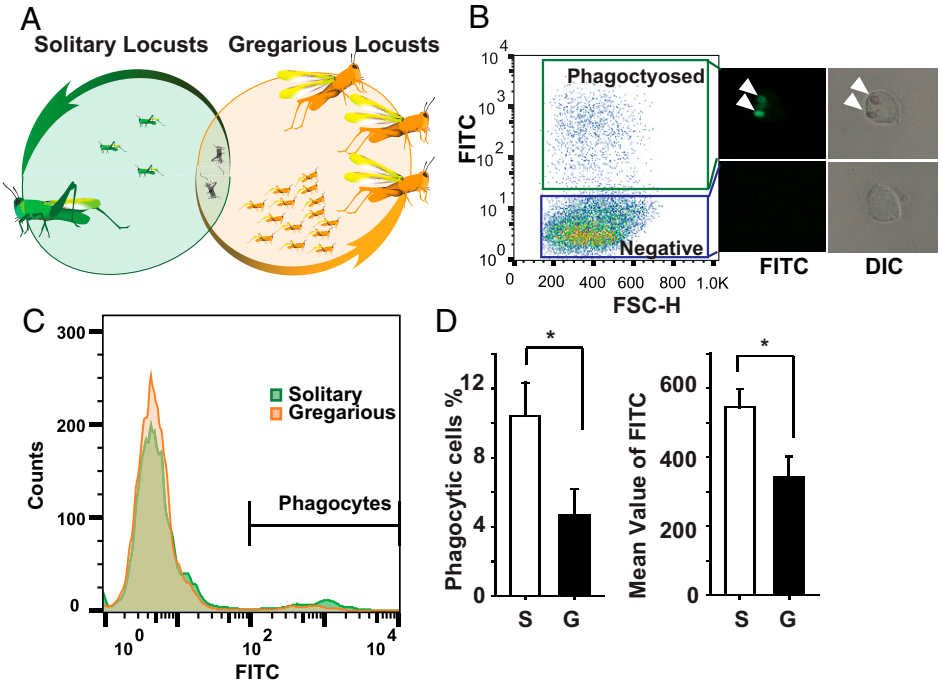

Fig. 2. Crowded locusts reduced phagocytosis to conidia of *M. anisopliae*. To investigate the effects of cellular defense in host resist high-virulence infection, we used the altered immunity of locust to observe the differential cellular defense between locust two phases. (*A*) Locust displays a reversible phase change between solitary and gregarious phases in response to low and high population density, respectively. Solitary and gregarious locusts. (*B*) For phagocytosis ability, phagocytic hemocytes of engulfing FITC-labeled conidia were successfully identified by flow cytometry. DIC: differential interference contrast. (*C*) The higher level of phagocytic cells was displayed in solitary locust than gregarious locusts after counting the positive hemocytes in the 10,000 cell counts. G: hemocytes sample of gregarious locusts; S: hemocytes sample of solitary locusts. (*D*) Proportion of phagocytic cells in gregarious locust was less than that of solitary locusts (*Right*, $n = 12$, $P < 0.001$), and showed lower capability of engulfing conidia (*Left*, $n = 12$, $P < 0.001$). Asterisk indicates the significance ($P < 0.01$).

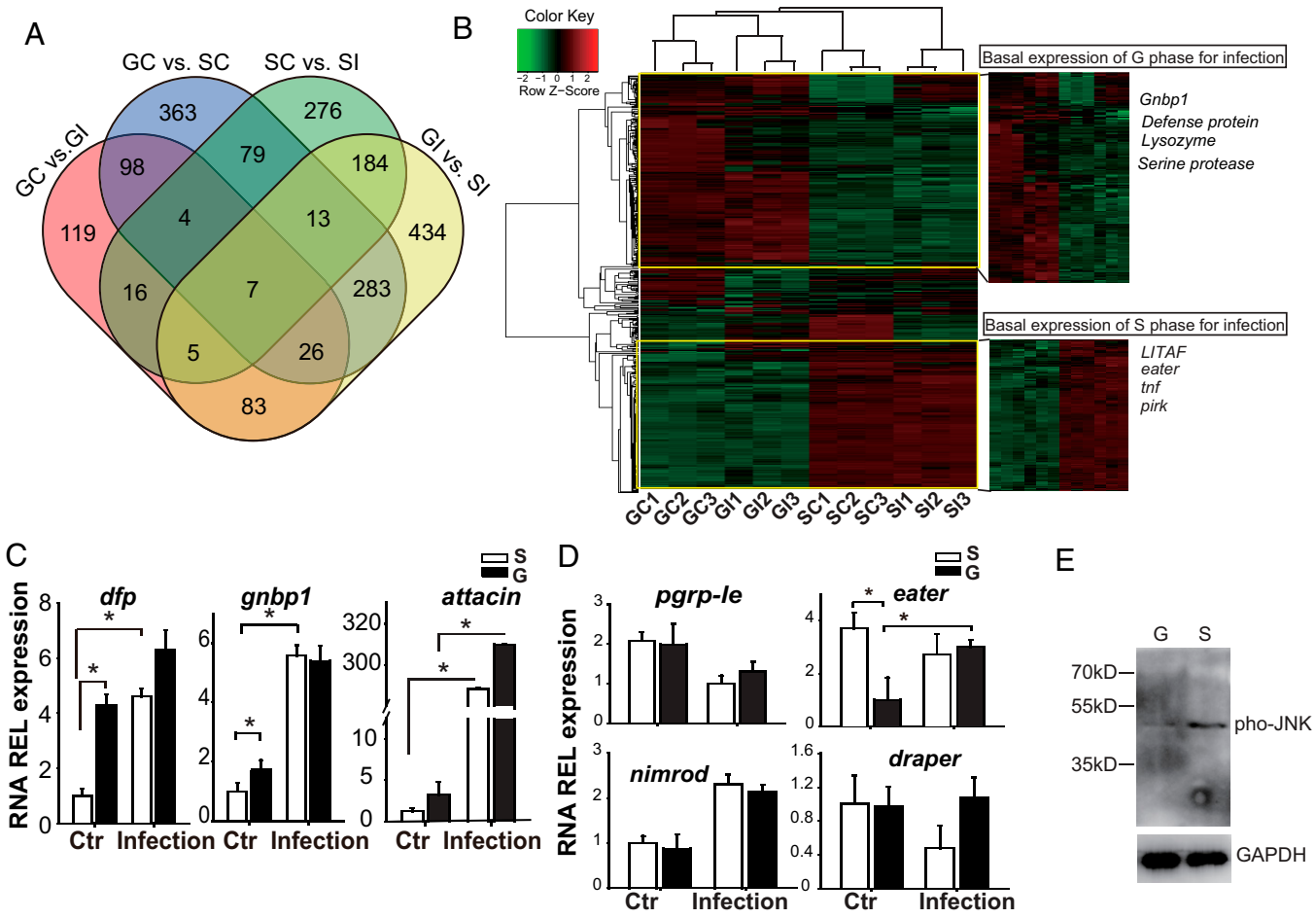

Fig. 3. Transcriptional analyzed the differential expression of hemocytes between solitary and gregarious locusts. (*A*) Venn diagram showed the distinct and shared transcripts for hemocytes of pre- and post- conidia infection between solitary and gregarious locusts. (*B*) Hierarchical analysis of differentially expressed genes (1,990 genes, adjust $P < 0.005$) of hemocytes before and after conidia infection showed the different defense strategies in the two locust phases. *Upper* box and *Lower* box indicates the distinct prophylactically expressed genes for resisting infection in hemocytes of gregarious and solitary locusts respectively. GC: control sample of gregarious locusts; SC: control sample of solitary locusts; GI: conidia-infected sample of gregarious locust; SI: conidia-infected sample of solitary locusts; *gnbp1*: gram-negative binding protein 1; *pirk*: poor Imd response upon knockin; *tnf*: tumor necrosis factor; (*C*) qPCR results indicated that gregarious locusts prophylactically expressed the effectors transcripts of *dfp* and *gnbp1* but not *attacin*. (*D*) qPCR results indicated that solitary locusts prophylactically expressed cytokine *tnf* and phagocytosis related receptor *eater*. Asterisk indicates the significance ($n = 12$, $P < 0.01$). (*E*) Immunoblot analysis of the differential activation of JNK phosphorylation in hemocytes of solitary and gregarious locusts. G: sample of gregarious locusts; S: sample of solitary locusts. Data presented as mean ± SEM.

proportion of phagocytic hemocytes ($n_G = 12$, $P_G = 0.0082$) and phagocytic capacity ($n_G = 12$, $P_G = 0.0105$) in gregarious locusts (Fig. 4*F*). Thus, TNF simultaneously regulated phagocytic receptors and immune effectors in solitary locusts.

TNF Optimized Locust Resistance against Fungal Infections. To determine the effects of TNF on locust survival after fungal infection, we altered TNF levels by TNF protein injection or RNA interference (RNAi) knockdown. Injection of additional TNF protein significantly reduced the mean lifespan of gregarious locusts from 8.1 ± 0.3–6.5 ± 0.3 d ($n_G = 49$, $P_{\text{LmTubulin vs. LmTNF}} = 0.001$) (Fig. 5*A*). On the contrary, reduced TNF by RNAi knockdown in the solitary locusts significantly increased the mean lifespan from 6.6 ± 0.3–7.5 ± 0.4 d after fungal infection ($n_S = 32$, $P_{\text{dsGFP vs. dsTNF}} = 0.013$) (Fig. 5*B*). However, reduced TNF levels in gregarious locusts and increased TNF levels in solitary locusts did not significantly affect their lifespan ($n_G = 48$, $P_{\text{LmTubulin vs. dsTNF}} = 0.287$; $n_S = 29$, $P_{\text{dsGFP vs. LmTNF}} = 0.616$). At low levels of TNF, phagocytosis of pathogens by hemocytes was inhibited, while pathogens were coated by high levels of effectors. However, high levels of TNF enhanced phagocytosis, and the escaped pathogens increased the risk of systemic infection (Fig. 5*C*). Thus, TNF plays an important role in balancing cellular and humoral defenses during locust adaptation to crowded conditions.

Discussion

In our study, the combination of mathematical models and experiments indicated that gregarious and solitary locusts employed different immune strategies of humoral defense or phagocytosis in response to infection by fungal pathogens. Although our previous research showed that gregarious locusts display high-level humoral defenses, mathematical simulation suggested that gregarious adopt high humoral defenses and require low cellular defenses to resist lethal fungal infection. Based on the differential cellular defenses between solitary and gregarious locusts, we found that TNF modulated the locust defense strategy switch in response to changes in the population density. These findings provide critical clues for understanding density-dependent prophylactic immunity and designing novel biopesticides for pest control.

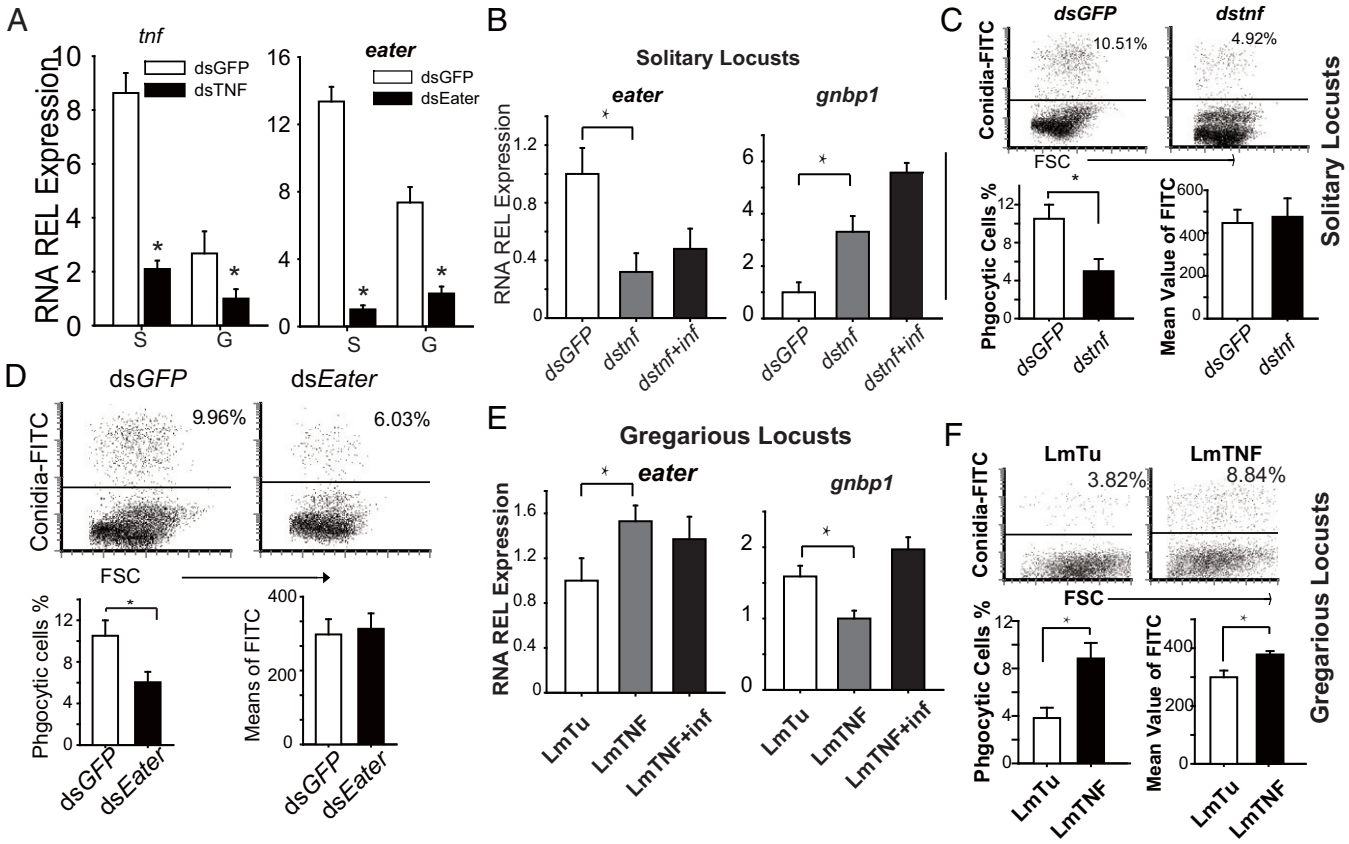

Fig. 4. Locust TNF simultaneously regulated the phagocytosis and effectors production. In hemocytes of locust, *(A)* mRNA expression level of *tnf* and *eater* can be significantly reduced by RNAi knockdown. (*B*) After reduced the locust TNF (*Lmtnf*) expression in solitary locusts, phagocytosis receptor *eater* was significantly decreased, while effector *gnbp1* expression was increased by qPCR analysis. (*C*) Flowcytometry results showed that knockdown *Lmtnf* expression by dsRNAi decreased the phagocytic hemocytes and did not affect the capability of phagocytosis in solitary locusts. (*D*) Flowcytometry results showed that knockdown *eater* expression by dsRNAi decreased the phagocytic hemocytes and did not affect the capability of phagocytosis in solitary locusts. (*E*) After injection of recombinant LmTNF, phagocytosis receptor *eater* was significantly increased while effector *gnbp1* expression was decreased by qPCR analysis in gregarious locusts. (*F*) Flowcytometry results showed that injection of LmTNF increased both the proportion of phagocytic hemocytes and the capability of phagocytosis in gregarious locusts. LmTu: locust Tubulin; LmTNF; locust TNF; inf: infection. Asterisk indicates the significance ($P < 0.01$). Data presented as mean ± SEM.

This stochastic simulation method provides an available approach to understand not only pathogen infections (29, 30) but also the altered immunity affected by environmental conditions. The model in this study predicted that hosts with immune status 3 with high humoral and high cellular defenses (high rate of phagocytosis) showed shorter survival times compared to hosts with immune status 6 (high humoral and low cellular defenses) after lethal pathogen infections. In fact, our results showed that gregarious locusts preferred high humoral and low cellular defenses to resist fungal infections. Other studies have shown that cellular defenses have deleterious effects on host defenses against intracellular pathogen infections (31, 32). After testing various parameters of pathogens, we found that humoral defenses dominated the host immune defenses, suggesting alternative results to previous research (15). Thus, gregarious locusts with high humoral and low cellular defenses showed a longer time to interact with pathogens, indicating a tolerant defense strategy in line with our previous research (3). Solitary locusts with high cellular defenses and low humoral defenses can rapidly remove nonlethal pathogen infections, providing an extended health time window for reproduction. Furthermore, the altered immunity of locusts in response to population density showed great potential to reveal host strategies for adaptation to environmental changes.

In this study, we confirmed that TNF modulates the locust defense strategy switch in response to changes in the population density. We observed that TNF played a role in regulating the altered immunity of locusts because transcriptome analysis of solitary and gregarious locusts showed variations in LITAF, which can induce TNF expression. We showed that TNF can significantly increase the phagocytic ability of hemocytes and suppress effector expression in solitary locusts. Low TNF levels in gregarious locusts allowed effector expression, including that of DFP and GNBP1. These effectors can initiate the encapsulation of pathogens (33) and degrade pathogen-associated molecular patterns (β-1,3-glucans) to attenuate the immune cascades for tolerance defense (3). However, we found that the gregarious locusts did not enhance AMP expression in the hemolymph, suggesting that the constitutive expression of AMPs is harmful to the limited resources of gregarious locusts because of the high cost of AMP production and the high concentration of AMPs required for killing pathogens (34). TNF is a metabolic hormone that inhibits animal growth by suppressing insulin production (21). The reduction in TNF levels can enhance not only the interactions between hosts and pathogens during infection but also the nutrition consumption for growth in animal life history.

By injecting recombinant TNF protein, we found that high levels of TNF protein significantly reduced the lifespan of

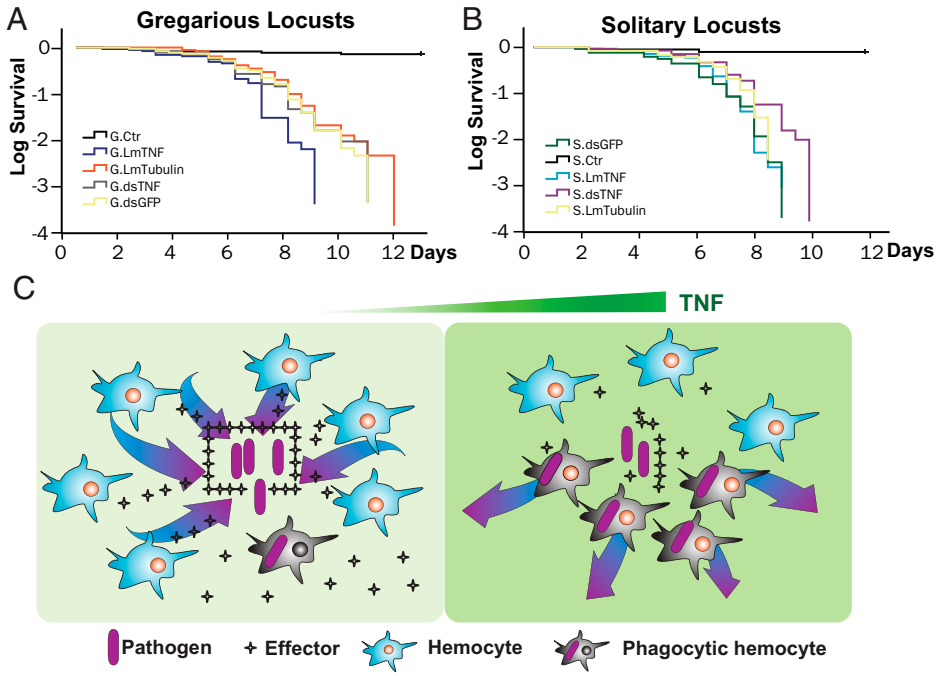

Fig. 5. TNF impaired locust defense against the infection of *M. anisopliae*. After changing the TNF expression level in locusts, the survival of locusts infected by fungi (*M. anisophilae*) was analyzed by Kaplan-Meier methods. (*A*) Increasing TNF level by injection of recombinant TNF proteins reduced the life span of gregarious locusts. ($n_G = 49$, $P_{LmTublin\ vs.\ LmTNF} = 0.001$). G.LmTubulin: gregarious locusts injected with recombinant tubulin protein; G.LmTNF: gregarious locusts injected with recombinant TNF protein; G.dsTNF: gregarious locusts reduced TNF expression by dsRNAi; G.ctr: gregarious locusts without fungal infections. (*B*) Knock down of TNF level by dsRNAi extended the life span of solitary locusts. ($n_S = 32$, $P_{dsGFP\ vs.\ dsTNF} = 0.013$). S.dsTNF: solitary locusts reduced TNF expression by dsRNAi; S.LmTNF: solitary locusts injected with recombinant TNF protein; S. dsGFP: solitary locusts injected with dsGFP; S.ctr: individuals of solitary locusts without fungal infections. (*C*) Schematic mechanisms showed that TNF affected host survival after pathogens infection. Low level of TNF ensured the effectors production and quarantined the pathogens to limit harmful effects. High level of TNF in solitary locusts enhanced the phagocytosis for pathogen clearance.

gregarious locusts. In control practice and laboratory bioassays, gregarious locusts always exhibit much stronger resistance to fungal pathogens than solitary locusts (2, 3). Gregarious locust swarms are the main control targets in field management practices. Because LPS from gram-negative bacteria can directly induce TNF expression by increasing the expression of LITAF (35), the gut microbiota for regulating host immunity may dominate the altered immunity of gregarious and solitary locusts. After investigation of the symbiont bacteria of locust, gregarious locusts adapted large amounts of gram-positive bacteria such as *Weissella* and *Enterococcus*, implying little LPS for induction of LITAF, whereas solitary locusts showed dominant gram-negative bacteria *Enterobacter* and *Betaproteobacteria* with sufficient LPS for LITAF induction (36–38). Interestingly, the use of bacteria for locust control has not continued since the 1950s (39). However, our evidence suggests that the use of a combination of bacteria and fungi to control gregarious locusts is a feasible approach. Our findings provide critical cues for understanding density-dependent prophylactic immunity and designing novel biopesticides for pest control.

Materials and Methods

Experimental Model. Migratory locusts were collected from the North China Plain (Huanghua, Hebei Province), and two locust phases were established as previously described (40). Gregarious locusts were reared in large, well-ventilated cages (25 cm × 25 cm × 25 cm) at densities of 200 to 300 insects per cage. Solitary locusts were individually reared under physical, visual, and olfactory isolation conditions using a ventilated cage (10 cm ×10 cm × 25 cm) with charcoal-filtered compressed air. These conditions maintained the phase traits required for reversible phase transition. Both gregarious and solitary cultures were reared under a 14:10 light/dark photoperiod at 30 ± 2 °C on a diet of fresh greenhouse-grown wheat seedlings and bran.

Kinetic Simulation. The kinetic process of microbial and hemocyte growth is shown as follows: N, number of hemocytes; M, number of microbes; Pha, number of phagocytes with microbes.

$N \rightarrow N + N$ (self-renew: α)
$M \rightarrow M + M$ (self-renew: β)
$M+N \rightarrow$ Pha (phagocytes ratio: K1)
Pha $\rightarrow$ M (microbe survival: K3)
Pha $\rightarrow$ N (hemocytes survival: K2)

The example program of simulation is listed in the *SI Appendix*, Table S4 for GillespieSSA R package.

Fungal Infection Assay. There are different forms of *M. anisopliae* in the life cycle during the infection of locusts, including 1) adhesion of conidia on the locust cuticle, 2) germination of the conidia and formation of an appressorium, 3) penetration of the germination tube through the cuticle into the hemocoel of locust, 4) production and multiplication of blastospores in the hemocoel, 5) mummified insect cadaver filled with mycelium of *M. anisopliae*, 6) outgrowth of hyphal strands, and 7) growth of conidiophores with conidia-building cells forming sterigmata.

To infect the locusts, we used male locust individuals after 4 d molting according to our previous study (3). Briefly, the locusts in the solitary and gregarious phases were inoculated with 2 μL peanut oil containing 1×10^6 conidia under the pronotum. This method is noninvasive, and peanut oil control has negligible effects on locusts. The locusts were reared under a 14:10 light/dark photoperiod at 30 ± 2 °C on a diet of fresh greenhouse-grown wheat seedlings and bran. The mortality of locusts was recorded twice daily. Survival curves were compared using the Kaplan-Meier method in SPSS13.0. Results were listed in *SI Appendix*, Table S5.

Chemicals. Unless otherwise indicated, the chemicals were obtained from Sigma-Aldrich. The recombinant cytokine TNF was dissolved in Leibovitz's L-15 culture medium at 100 ng/mL, and injected at 200 pg per locust. Other raw materials, including plasmids, PCR primers, and antibodies, are shown in *SI Appendix*, Table S6.

Flow Cytometry Assay. Four days after molting, locust individuals were injected according to modified procedures. In brief, locusts from each phase were injected with 2 μL of Leibovitz's L-15 medium containing 1×10^8 heat-killed conidia (*M. anisopliae*, FITC-labeled) into the hemocoel in the second ventral segment of the abdomen, and L-15 medium served as the control. Hemocytes were collected 3 h after the conidia were injected. The 10 μL of hemolymph was rapidly collected into 1.0 mL precooled L-15 media. Before loading on a BD Calibur analyzer, the hemolymph was centrifuged at 400 g for 5 min and then suspended in the 200 μL cell pallet in L-15 media. Control and positive samples were used for calibration. A total of 10,000 hemocytes from each sample were counted to evaluate phagocytosis. The results were analyzed using software FCS express 4.0 and FlowJo ×.

Recombinant Protein Production. Proteins for injection were expressed in *Escherichia coli* (locust TNF domain: nucleotides 374–826, GenBank accession: KP233713, locust Tubulin domain: nucleotides 152–811, GenBank accession: KP844460) using the Invitrogen pET-28a vector. The proteins were purified with Ni-Sepharose (GE Healthcare) and polished by gel filtration with CM-25 Sephadex in locust saline buffer before injection. After determining the protein concentration by the BCA assay, each locust was injected with 20 ng of target proteins.

Cell Culture. The macrophage cell line RAW 264.7 was used to examine the expression of TNF regulated by adenosine. Because the cells were cultured in RPMI 1640 with 10% fetal bovine serum containing adenosine, we used 35 μM adenosine to stimulate the responses of mouse cells. To investigate the stable effects of extracellular adenosine, 2-chloroadenosine and NMBPR (70 μM) were used to observe the responses of macrophages. Because of the toxicity of 2-chloroadenosine, we used a concentration of 3.5 μM to observe the cellular response. After seeding the cells in 6-well plates overnight, drugs were added to the culture. After 6 h, RPMI1640 without fetal bovine serum was used to wash the cells. Next, 1 mL of TRIzol was added to the wells to lyse the cells. According to the TRIzol manufacturer's instructions, RNA and proteins from cells were extracted for further analysis.

RNA-Sequencing Experiments. We used a high-throughput sequencing platform (HiSEq. 2500) to analyze the expression of genes in the hemocytes of pre- and postinfected gregarious and solitary locusts. Four days after infection with fungal conidia (*M. anisopliae*) or peanut oil, three replicates (15 individuals per replicate) of each sample were collected for analysis. Total RNA was extracted using TRIzol (Life Sciences), and purity was examined. Following, 2–5 μg messenger RNA (mRNA) was purified using magnetic beads, according to the manufacturer's instructions (Illumina). After high-throughput paired-end sequencing, the raw reads were aligned using Bowtie software, and abundance estimation was performed as previously described. Differentially expressed transcripts were analyzed using DESeq. The locust reference genome and gene functional analyses were performed using methods described in previous research (3, 10). Raw reads of the four samples were downloaded from the NCBI SRA server (accession number: SRA072524).

Quantitative PCR Analysis. To observe the expression of target genes, qPCR was performed in accordance with the standard protocols for thermocyclers (Roche). At least three biological replicates (four individuals per replicate) were pooled for the analysis of three parallel technical replicates. The mRNA of each sample was extracted from the hemolymph using TRIzol reagent (Life Sciences). The OD_{260}/OD_{280} ratios were then measured. cDNA was synthesized from 2 μg total RNA using an MLV reverse II system (Promega). The primers used are shown in the *SI Appendix*). The *actin* sequence of *L. migratoria* (GenBank accession: AF370793) was used as an internal control and the target gene sequences were cloned into pGEM-T Easy for standard curve calibration. The specificity of amplification was confirmed by melting curve analysis.

dsRNAi Experiments. We used the double-stranded RNA mediated interference (dsRNAi) method to knock down target gene expression. The templates for dsRNA preparation were PCR-derived fragments between the two T7 promoter sequences. The fragments of each gene were as follows: *gfp* (nucleotides ORF35-736, GenBank accession: L29345), Locust *tnf* (nucleotides 128–829, GenBank accession: KP233713), and *eater* (nucleotides 442–904, GenBank accession: KP233712). Single-stranded RNA fragments were synthesized using a T7 Transcription Kit (Promega). The annealed dsRNA was purified by ethanol precipitation and dissolved in sterilized L-15 medium buffer at 5 μg/μL until use. Finally, each insect was injected with 20 μg dsRNA for the experiments.

Immunoblot Assay. Hemocyte proteins were extracted from TRIzol samples after RNA preparation. After extraction, the protein pellets were dried at room temperature for ~12 h. Proteins were then weighed and dissolved in rehydration buffer without ampholytes (Bio-Rad) at a concentration of 20 μg/μL. Following, 100 μg of proteins per lane was separated using SDS-PAGE and transferred to a PVDF membrane (Life Sciences). After blocking with 5% skimmed milk, the primary antibody was diluted to 1:1,000 and incubated overnight at 4 °C. The secondary antibody (A1949, Sigma) was used to detect the primary antibody at a 1:12,000 dilution and visualized by chemiluminescence (Thermo) in a Transilluminator OUS (Carestream).

Statistical Analysis. For all qPCR results, the data are presented as mean ± SEM, and the *P* values were calculated using the Mann–Whitney *U* test provided by SPSS 13.0. Other methods for calculating significance are specified in the figure legends.

Data Availability. All study data are included in the article and/or *SI Appendix*.

ACKNOWLEDGMENTS. We thank Drs. Xian C. Li, Hong Zhang, and Dr. Zhen Zou for commenting on and revising the earlier version of the manuscript. We are particularly grateful to the anonymous reviewers, who provided useful comments and suggestions for improving our manuscript. This research was supported by the Strategic Priority Research Program of the Chinese Academy of Sciences (XDB11010000), the China Postdoctoral Science Foundation (2013M530765), and the National Natural Science Foundation of China (31670420).

1. J. Rolff, M. T. Siva-Jothy, Invertebrate ecological immunology. *Science* **301**, 472–475 (2003).
2. K. Wilson *et al.*, Coping with crowds: Density-dependent disease resistance in desert locusts. *Proc. Natl. Acad. Sci. U.S.A.* **99**, 5471–5475 (2002).
3. Y. Wang, P. Yang, F. Cui, L. Kang, Altered immunity in crowded locust reduced fungal (Metarhizium anisopliae) pathogenesis. *PLoS Pathog.* **9**, e1003102 (2013).
4. X. H. Wang, L. Kang, Molecular mechanisms of phase change in locusts. *Annu. Rev. Entomol.* **59**, 225–244 (2014).
5. P. Brodin *et al.*, Variation in the human immune system is largely driven by non-heritable influences. *Cell* **160**, 37–47 (2015).
6. B. P. Lazzaro, J. Rolff, Immunology. Danger, microbes, and homeostasis. *Science* **332**, 43–44 (2011).
7. A. I. Tauber, *Immunity: The Evolution of an Idea* (Oxford University Press, New York, NY, 2017).
8. W. Guo, X. H. Wang, D. J. Zhao, P. C. Yang, L. Kang, Molecular cloning and temporal-spatial expression of I element in gregarious and solitary locusts. *J. Insect Physiol.* **56**, 943–948 (2010).
9. R. Wu *et al.*, Metabolomic analysis reveals that carnitines are key regulatory metabolites in phase transition of the locusts. *Proc. Natl. Acad. Sci. U.S.A.* **109**, 3259–3263 (2012).
10. X. Wang *et al.*, The locust genome provides insight into swarm formation and long-distance flight. *Nat. Commun.* **5**, 2957 (2014).
11. M. Yang *et al.*, miR-71 and miR-263 jointly regulate target genes chitin synthase and chitinase to control locust molting. *PLoS Genet.* **12**, e1006257 (2016).
12. G. A. Miller, S. J. Simpson, Isolation from a marching band increases haemocyte density in wild locusts (Chortoicetes terminifera). *Ecol. Entomol.* **35**, 236–239 (2010).
13. J. G. King, J. F. Hillyer, Infection-induced interaction between the mosquito circulatory and immune systems. *PLoS Pathog.* **8**, e1003058 (2012).
14. J. G. King, J. F. Hillyer, Spatial and temporal in vivo analysis of circulating and sessile immune cells in mosquitoes: Hemocyte mitosis following infection. *BMC Biol.* **11**, 55 (2013).
15. N. Matova, K. V. Anderson, Rel/NF-kappaB double mutants reveal that cellular immunity is central to Drosophila host defense. *Proc. Natl. Acad. Sci. U.S.A.* **103**, 16424–16429 (2006).
16. B. Charroux, J. Royet, Elimination of plasmatocytes by targeted apoptosis reveals their role in multiple aspects of the Drosophila immune response. *Proc. Natl. Acad. Sci. U.S.A.* **106**, 9797–9802 (2009).
17. D. Sims, P. Duchek, B. Baum, PDGF/VEGF signaling controls cell size in Drosophila. *Genome Biol.* **10**, R20 (2009).
18. A. Rajan, N. Perrimon, Drosophila cytokine unpaired 2 regulates physiological homeostasis by remotely controlling insulin secretion. *Cell* **151**, 123–137 (2012).
19. F. Lombardo, Y. Ghani, F. C. Kafatos, G. K. Christophides, Comprehensive genetic dissection of the hemocyte immune response in the malaria mosquito Anopheles gambiae. *PLoS Pathog.* **9**, e1003145 (2013).
20. S. Tsuzuki *et al.*, Switching between humoral and cellular immune responses in Drosophila is guided by the cytokine GBP. *Nat. Commun.* **5**, 4628 (2014).
21. N. Agrawal *et al.*, The Drosophila TNF Eiger is an adipokine that acts on insulin-producing cells to mediate nutrient response. *Cell Metab.* **23**, 675–684 (2016).
22. T. Igaki *et al.*, Eiger, a TNF superfamily ligand that triggers the Drosophila JNK pathway. *EMBO J.* **21**, 3009–3018 (2002).

23. L. S. Garver, G. de Almeida Oliveira, C. Barillas-Mury, The JNK pathway is a key mediator of Anopheles gambiae antiplasmodial immunity. *PLoS Pathog.* **9**, e1003622 (2013).
24. H. Weavers, I. R. Evans, P. Martin, W. Wood, Corpse engulfment generates a molecular memory that primes the macrophage inflammatory response. *Cell* **165**, 1658–1671 (2016).
25. J. J. Gillard, T. R. Laws, G. Lythe, C. Molina-París, Modeling early events in Francisella tularensis pathogenesis. *Front. Cell. Infect. Microbiol.* **4**, 169 (2014).
26. D. T. Gillespie, Stochastic simulation of chemical kinetics. *Annu. Rev. Phys. Chem.* **58**, 35–55 (2007).
27. M. Pineda-Krch, S. S. A. Gillespie, Implementing the Gillespie stochastic simulation algorithm in R. *J. Stat. Softw.* **25**, 1–18 (2008).
28. L. Wang, Z. Feng, X. Wang, X. Wang, X. Zhang, DEGseq: An R package for identifying differentially expressed genes from RNA-seq data. *Bioinformatics* **26**, 136–138 (2010).
29. E. L. Read, A. A. Tovo-Dwyer, A. K. Chakraborty, Stochastic effects are important in intrahost HIV evolution even when viral loads are high. *Proc. Natl. Acad. Sci. U.S.A.* **109**, 19727–19732 (2012).
30. C. L. Althaus, R. J. De Boer, Intracellular transactivation of HIV can account for the decelerating decay of virus load during drug therapy. *Mol. Syst. Biol.* **6**, 348 (2010).
31. D. S. Schneider *et al.*, Drosophila eiger mutants are sensitive to extracellular pathogens. *PLoS Pathog.* **3**, e41 (2007).
32. A. Thakur, H. Mikkelsen, G. Jungersen, Intracellular pathogens: Host immunity and microbial persistence strategies. *J. Immunol. Res.* **2019**, 1356540 (2019).
33. Y. Y. Bao *et al.*, An immune-induced reeler protein is involved in the Bombyx mori melanization cascade. *Insect Biochem. Mol. Biol.* **41**, 696–706 (2011).
34. M. N. Melo, R. Ferre, M. A. Castanho, Antimicrobial peptides: Linking partition, activity and high membrane-bound concentrations. *Nat. Rev. Microbiol.* **7**, 245–250 (2009).
35. X. Tang, D. Metzger, S. Leeman, S. Amar, LPS-induced TNF-alpha factor (LITAF)-deficient mice express reduced LPS-induced cytokine: Evidence for LITAF-dependent LPS signaling pathways. *Proc. Natl. Acad. Sci. U.S.A.* **103**, 13777–13782 (2006).
36. S. Yuan, Y. Wang, F. Zhao, L. Kang, Complete genome sequence of *Weissella confusa* LM1 and comparative genomic analysis. *Front. Microbiol.* **12**, 749218 (2021).
37. O. Lavy, U. Gophna, E. Gefen, A. Ayali, The effect of density-dependent phase on the locust gut bacterial composition. *Front. Microbiol.* **9**, 3020 (2019).
38. O. Lavy, U. Gophna, E. Gefen, A. Ayali, Locust bacterial symbionts: An update. *Insects* **11**, 655 (2020).
39. B. Zelazny, M. S. Goettel, B. Keller, The potential of bacteria for the microbial control of grasshoppers and locusts. *Mem. Entomol. Soc. Can.* **129**, 147–156 (2012).
40. Z. Ma, W. Guo, X. Guo, X. Wang, L. Kang, Modulation of behavioral phase changes of the migratory locust by the catecholamine metabolic pathway. *Proc. Natl. Acad. Sci. U.S.A.* **108**, 3882–3887 (2011).